UCRL-JC-127575
PREPRINT

Demonstration of Enhanced Warhead Performance with More Powerful Explosives

Michael J. Murphy, Dennis Baum, Randall L. Simpson (LLNL)
Joe Monolo/NSWC Dahlgren
Lou Montesi/NSWC Dahlgren
Kirk Newman/NSWC Yorktown
Dieter Tuerpe/Primex Technologies
John Osborn/Orlando Technology

This paper is prepared for submittal to the
Ballistics 98, 17th International Symposium on Ballistics
Midrand, South Africa 23-27 March 1998

December, 1997

Lawrence Livermore National Laboratory

DEMONSTRATION OF ENHANCED WARHEAD PERFORMANCE WITH MORE POWERFUL EXPLOSIVES[1]

Michael J. Murphy (1), Dennis W. Baum (1), Randall L. Simpson (1), Joe Monolo (2a), Lou Montesi (2a), Kirk Newman (2b), Dieter Tuerpe (3), John Osborn (4)

(1) Lawrence Livermore National Laboratory, P.O. Box 808, L-282, Livermore, CA
(2) Naval Surface Warfare Center, (a) Dahlgren , (b) Yorktown
(3) Primex Technologies (formerly Physics International), San Leandro, CA
(4) Orlando Technology, Inc, Shalomar, FL

Enhanced warhead performance has been demonstrated for several warhead configurations loaded with more powerful explosives. This paper presents experimental results from several warheads loaded with one of the new more powerful explosives, LX-19. The LX-19 formulation is a volume analog to LX-14 (HMX/Estane) that consists of 95.8 wt. % epsilon CL-20 formulated with 4.2 wt. % Estane binder. The LX-19 formulation, characterization, and evaluation efforts presented in this paper are the result of several studies that have been ongoing since 1991. The warhead configurations that have been tested include a trumpet lined shaped charge, a hemispherical lined shaped charge, an EFP charge, and a fragmentation warhead. Performance improvements have been demonstrated with all configurations that were tested.

INTRODUCTION

It is common knowledge that three very important properties of a directed energy munitions are fabrication precision, liner properties, and explosive power. In the last 20 years, improvements in the first two have lead to demonstrations of increased warhead performance. Unfortunately, less has been done in the area of explosive power because new, more powerful explosives with acceptable safety and cost do not come along very often. The three most common energetic molecules used in munitions, TNT, RDX, & HMX were discovered in about 1850, 1900, and 1950, respectively. Thus, it was quite exciting when A. Nielson [1] first synthesized CL-20 in the late 1980's. The explosive performance of the epsilon phase [2] of this material was found by LLNL to be approximately 14% greater than HMX as determined by cylinder expansion and tantalum plate acceleration experiments making it the most powerful explosive ever tested at small volume expansions of the detonation products [3]. This prompted us to formulate LX-19 (formerly called RX-39-AB and RX-39-AC) as a baseline material for warhead evaluations. LX-19 is a volume analog to LX-14 (HMX/Estane) that consists of 95.8 wt. % epsilon CL-20 with 4.2 wt. % Estane binder. The LX-19 formulation, characterization, and shaped charge, hemispherical charge, explosively formed projectile (EFP) charge, and fragmentation warhead evaluation efforts presented in this paper are the result of several studies that have been ongoing since 1991.

[1] Work performed under the auspices of the U.S. Department of Energy by the Lawrence Livermore National Laboratory under Contract W-7405-Eng-48.

LX-19 PROPERTIES

LX-19 is a conventional plastic bonded explosive consisting of epsilon-phase CL-20 (2,4,6,8,10,12-hexanitro-2,4,6,8,10,12-hexaazaisowurtzitane) formulated with an Estane-based binder. The CL-20 starting material has a median size of 160 µm of which 25% percent is ground to 6 µm and reblended to produce a material that can be pressed to a high percent of the theoretical maximum density. All of the formulations were made by dissolving the Estane in $EtCl_2$, adding the CL-20 to the lacquer, and then removing the solvent under vacuum.

Small Scale Safety

CL-20 impact sensitivity is similar to PETN, however, formulated materials are significantly less sensitive with the impact values approaching those of HMX-based formulations. A comparison of small scale safety test results for LX-14 and LX-19 is given in Table 1.

Table 1. Small scale safety test results.

Material	Impact (cm)[a]	Friction(kg)[b]	Spark[c]	CRT(cm^3/g)[d]
LX-14	53	-	no reaction	0.08
LX-19	40	11.2-14.4	no reaction	0.136

[a] 2.5 kg Type 12 tool with 35 mg pressed samples.

[b] Julius-Peters-Berlin 21 friction machine. One reaction in ten tries.

[c] Ten tries at 1J with 510 ohm in line resistance.

[d] 2 hours at 120°C under 1 atm He.

Performance Test Results

A cylinder test (25.4 mm diameter, 2.54 mm thick copper wall), five tantalum-plate acceleration experiments, and three particle-velocity measurements using NaCl crystals have been conducted on LX-19 (RX-39-AB) by LLNL [4,5]. The results of the LX-19 Ta plate push experiments are compared to LX-14 in Figures 1a & 1b [3]. These test results show that LX-19 significantly out performs LX-14 over the entire range of expansion.

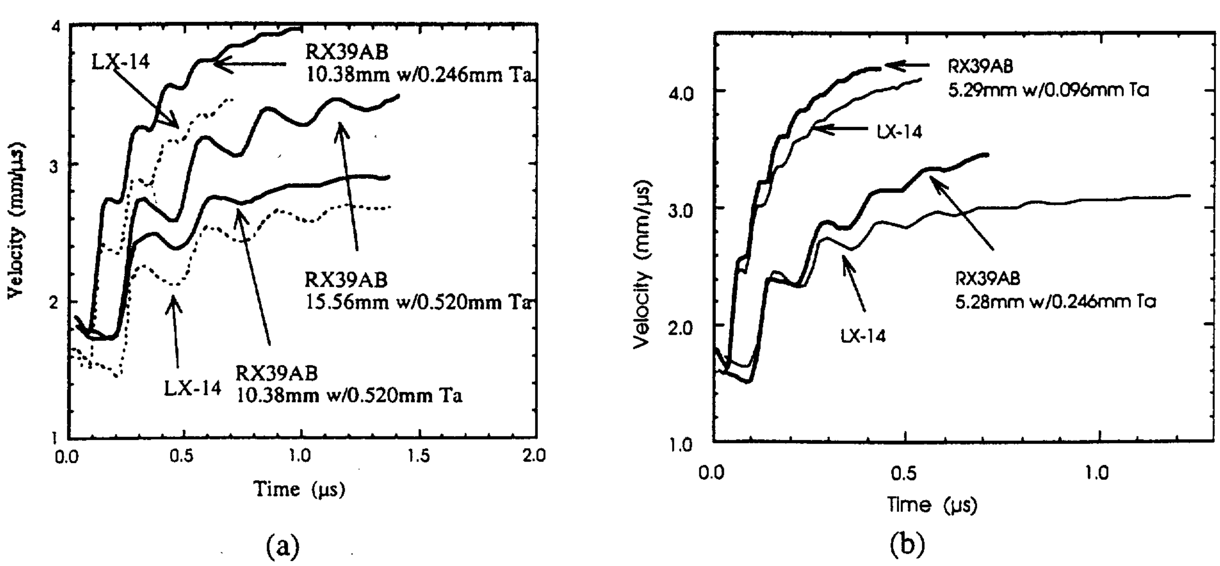

Fig. 1a & 1b Ta plate push experiments for LX-19 (RX-39-AB) and LX-14 [3].

Equation of State

The JWL EOS parameter values for LX-19 at three different densities are given in Table 2. The 1.942 gm/cc density EOS is based on cylinder test data while the other two are derived from Cheetah [6] calculations and scaling from the 1.942 gm/cc EOS. The cylinder test experiment was loaded with several 25.4 mm diameter by 25.4 mm long pressed cylinders of LX-19. The combination of a length/diameter ratio of unity and optimum pressing conditions resulted in a pressed part TMD of 98.1%. The 1.920 g/cc density is more consistent with the density of the loaded warheads we tested.

Table 2. JWL equation of state parameters for LX-19 at different densities.

Parameter	LX-19 (1.900)	LX-19 (1.920)	LX-19 (1.942)
ρ_0 (g/cm^3)	1.900	1.920	1.942
% TMD	96.0	97.0	98.1
P_{CJ} (100 GPa)	0.400	0.415	0.430
D (cm/μs)	0.9000	0.9104	0.9208
E_0 (100GPa-cm^3/cm^3)	0.1126	0.1133	0.1150
A (100 GPa)	15.7195	15.9665	16.3795
B (100 GPa)	1.6723	1.7741	1.8629
R_1	6.5	6.5	6.5
R_2	2.7	2.7	2.7
ω	0.55	0.55	0.55

TRUMPET LINED SHAPED CHARGE

The first warhead we tested with the LX-19 material is described in Fig. 2. This device has a lightly confined cylindrical body with a trumpet shaped liner. Since this precision warhead had been previously tested with Octol and LX-14, it was considered a good warhead for evaluation of the new LX-19 formulation. This shaped charge warhead has a precision initiation coupler (PIC) initiator, lightly confined aluminum body and a copper liner. The LX-19 was pressed to shape using the same tooling that was used for LX-14 at about the same pressing conditions. The liner was bonded to the pressed LX-19 billet, which was bonded into the aluminum body. One x-ray experiment and 10 penetration experiments were conducted.

X-ray Experiment

The X-ray test was used to determine the characteristics of the jet. From the jet tip down to a velocity of 5 km/sec, the LX-19 jet had about 30% more mass than the LX-14 jet. Data for the Octol jet was not available. The LX-19 jet breakup time was 10% greater than for the Octol jet and 6% greater than for the LX-14 jet.

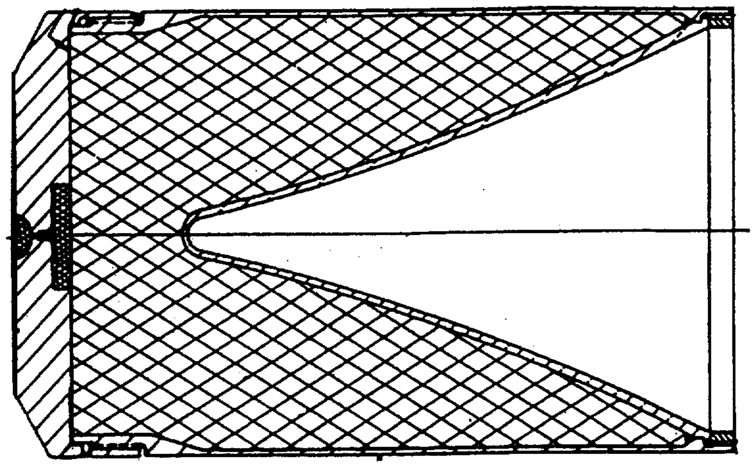

Fig. 2. General description of the trumpet lined shaped charge.

Penetration Experiments

The results of the jet penetration experiments for LX-19, Octol, and LX-14 are shown in Fig. 3. The penetration data for the LX-19 (triangles) consisted of two experiments at each of five standoffs. This figures shows a big increase in penetration over Octol (squares) at longer standoffs and a fairly consistent increase in penetration over LX-14 (diamonds) at all standoffs. The small penetration increase at the short standoff is because most of the penetration occurs prior to jet breakup and the influence of an increased jet breakup time is not realized.

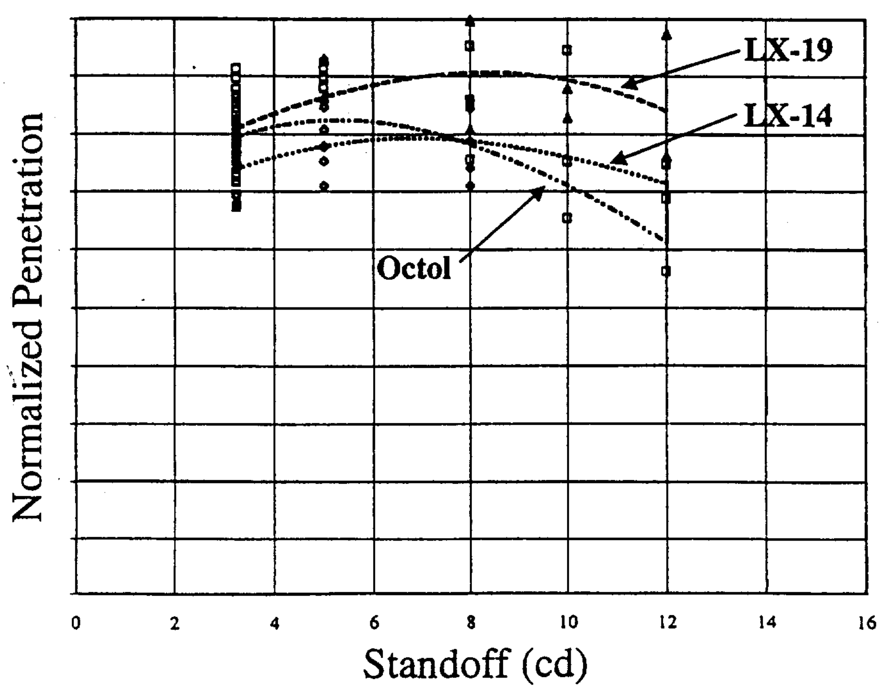

Fig. 3. Relative jet penetration versus standoff for Octol, LX-14, and LX-19.

HEMISPHERICAL LINED SHAPED CHARGE

A general description of the hemispherical lined shaped charge is shown in Fig. 4. This charge was loaded and tested with LX-14 and LX-19. The explosives were pressed to near net shape and then machined to match the contour of the body and copper liner. The charge was lightly confined. Long standoff x-rays of the jets from both explosives were taken with the results described in the figures below. A comparison of the normalized jet length versus jet velocity for the two explosives is given in Fig. 5. This figure shows that from the jet tip to about 3 km/sec, the LX-19 loaded warhead created a jet with about a 50% greater length than the LX-14 jet. A comparison of the normalized jet breakup time (breakup time divided by charge diameter) is given in Fig. 6. This figure shows why the LX-19 jet was much longer than the LX-14 jet. The LX-19 jet had up to a 50% increase in jet breakup time compared to the LX-14 jet. Some of the large increase in jet length with LX-19 that is observed in Fig. 5 can be attributed to the decrease in jet breakup time with the LX-14 at about 3 km/sec. This may be an experimental anomaly. However, it is clear that the LX-19 jet was much longer with a greater breakup time.

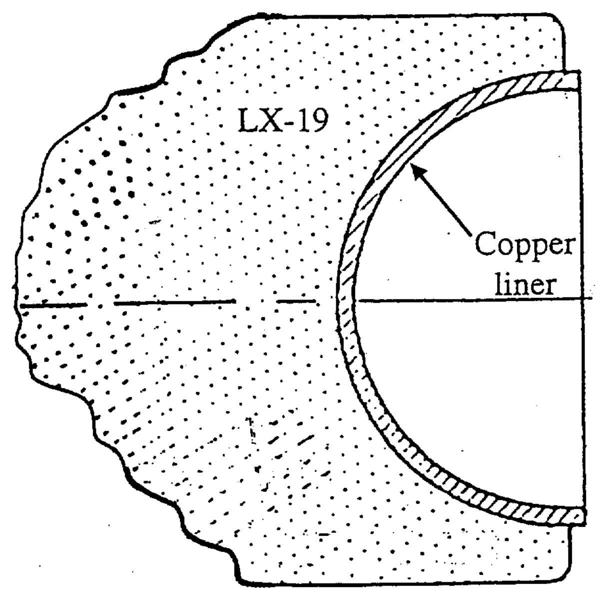

Fig. 4. General description of the hemispherical lined shaped charge.

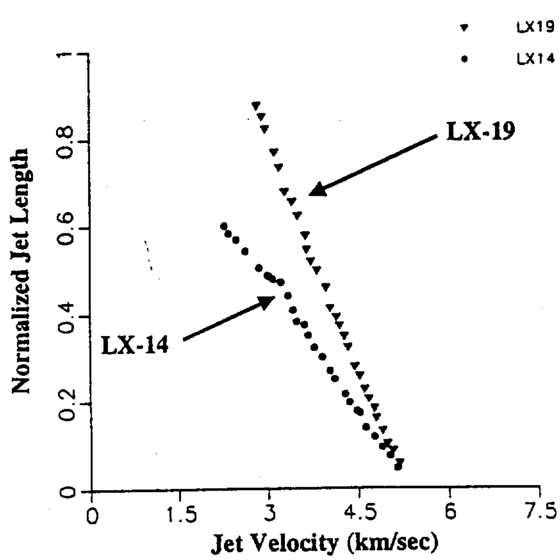

Fig. 5 Normalized jet length versus jet velocity for LX-14 and LX-19.

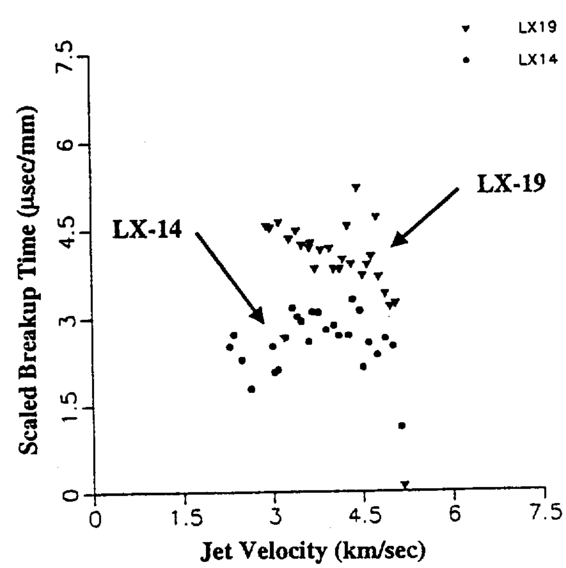

Fig. 6 Scaled jet breakup time versus jet velocity for LX-14 and LX-19.

EXPLOSIVELY FORMED PROJECTILE WARHEAD

A general description of the explosively formed projectile (EFP) warhead is given in Fig. 7. An X-ray shadowgraph image of the EFP is shown in Fig. 8 [7]. This EFP warhead has been used for previous liner material studies [8, 9, and 10]. A comparison of the LX-14 and LX-19 calculated and experimental EFP velocity and EFP length are given in Table 3. The EFP velocity data is normalized to the LX-14 EFP experiment. The EFP length data is also normalized to the LX-14 experiment.

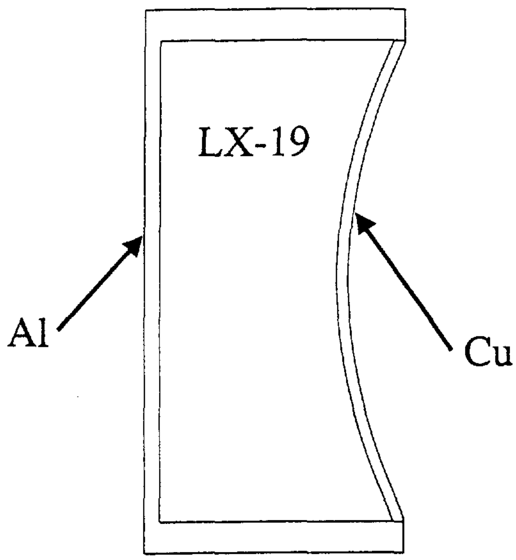

Fig. 7. Description of the EFP warhead.

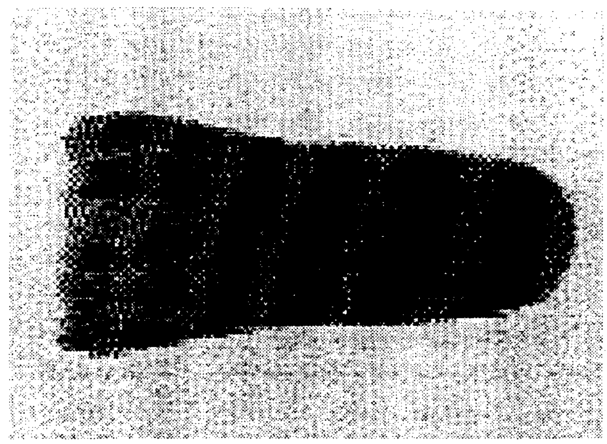

Fig. 8 X-Ray of the EFP projectile.

EFP velocity

The table below shows the LX-19 EFP had a 7% greater velocity (14% greater energy) than the LX-14 projectile. The calculated EFP velocity using the 1.942 g/cc JWL EOS given in Table 2 was exactly the same as the value from the experiment.

EFP length

Although our calculations were correct for the EFP velocities, we were about 5% off on the EFP lengths. Our predictions were about 5% under length for LX-14 and 5% over length for LX-19. Since the LX-19 projectile was shorter than the LX-14 projectile, we feel there may be some experimental error or uncertainty with the length data.

Table 3. Comparison of LX-14 and LX-19 EFP velocity and EFP length.

		LX-14	LX-19
Experimental EFP velocity	(normalized)	1	1.07
Calculated EFP velocity	(normalized)	1.00	1.07
Experimental EFP Length	(normalized)	1	0.95
Calculated EFP Length	(normalized)	0.95	1.00

FRAGMENTATION WARHEAD

A general description of the fragmentation warhead is given in Fig. 9. This device was loaded with both Comp-A5 and LX-19. The explosives were first pressed directly into the fragmentation body. The liner was then pressed into the explosive and crimped to the body. The fragmentation pattern used in the interior of the body was a 58° rhombus. A comparison of the normalized experimental results with the two explosives is given in Table 4. The table shows that LX-19 produced a 7% increase in fragment velocity compared to Comp A5. In spite of the 58° rhombus fragmentation pattern, the LX-19 produced a 71% increase in the number of fragments with a corresponding decrease in the mass of each fragment. The LX-19 also provided a 2% increase in penetration at the less than 1 CD built-in standoff.

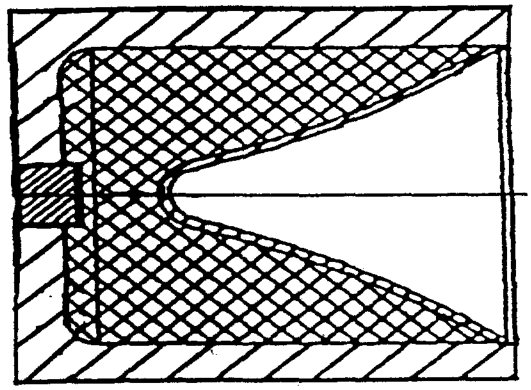

Fig. 9 General description of the fragmentation warhead.

Table 4. Comparison of fragmentation test results using Comp A5 and LX-19.

	Comp A5	LX-19
ρ_o (g/cm^3)	1.65	1.92
P_{CJ} (100 GPa)	0.300	0.415
D (mm/μs)	8.300	9.104
Relative fragment velocity	1	1.07
Relative number of fragments	1	1.71
Relative fragment mass	1	0.59
Relative jet penetration	1	1.02

CONCLUSIONS

LX-19 is one of the most powerful metal pushing explosives that we have ever tested. When loaded in a shaped charge, hemi charge, EFP charge and fragmentation charge it produced performance improvements when compared to Octol, LX-14, and Comp A6. It is our opinion that more powerful explosives are a vital component in the three P's (fabrication precision, liner properties, and explosive power) of directed energy munitions.

ACKNOWLEDGEMENTS

The information presented in this paper is the result of the efforts of many individuals and many organizations. A special acknowledgement goes to the Joint DoD/DOE Munitions Technology Development Program for their initial funding on the HE work and warhead evaluations.

REFERENCES

1. A. Nielsen, Polycyclic Amine Chemistry in: G.A. Olah and D.R. Squire, (eds), Chemistry of Energetic Materials, , Academic Press, San Diego, 1991, pp. 95-124.
2. Epsilon-CL-20, synthesized by Gencorp Aerojet.
3. R.L. Simpson, P.A. Urtiew, D.L. Ornellas, G.L. Moody, K.J. Scribner and D.M. Hoffman, CL-20 Performance Exceeds That Of HMX And Its Sensitivity Is Moderate, Propellants, Explosives, Pyrotechnics, 22, 249-255 (1997).
4. (4) J.W. Kury, H.C. Hornig, E.L. Lee, J.L. McDonnel, D.L. Ornellas, M. Finger, F.M. Strange, M.L. Wilkens," Ninth Symp. (International) on Detonation, White Oak, Oct. 12-15, 1965, pp. 3-13.
5. P.C. Souers, B. Wu, L.C. Haselman, Jr., "Detonation Equation of State at LLNL, 1995, LLNL Report UCRL-ID-119262 Rev 3., Feb. 1996.
6. B. Travers, Experimantal result of LX-19 EFP experiment conducted by U.S. Army ARDEC, private communication, 1993.
7. Fried, Cheetah
8. Murphy, M. J., Constitutive model parameter determination from generic EFP warhead tests", J de Physique IV, Colloque C8, Vol 4, 483, 1994.
9. Murphy, M. J., Baker, E. L., Using nonlinear optimization methods to reverse engineer liner material properties from EFP tests", 15th Int Symp on Ballistics, 1995.
10. Murphy, M. J, Lassila, D.H., Modeling and Evaluation of HE Driven Shock Effects In Copper with the MTS Model, J de Physique IV, Colloque C3, Vol 7, 655, 1997.

Technical Information Department **• Lawrence Livermore National Laboratory**
University of California • Livermore, California 94551